Radiation Physics and Chemistry 147 (2018) 70–76

Contents lists available at ScienceDirect

Radiation Physics and Chemistry

journal homepage: www.elsevier.com/locate/radphyschem

Neutron sensitivity of ^{6}Li-based suspended foil microstrip neutron detectors using Schott Borofloat® 33 microstrip electrodes

Nathaniel S. Edwards[a,*], Benjamin W. Montag[a,b], Luke C. Henson[b], Steven L. Bellinger[a,b], Daniel M. Nichols[a], Michael A. Reichenberger[a], Ryan G. Fronk[a], Douglas S. McGregor[a]

[a] S.M.A.R.T. Laboratory, Department of Mechanical and Nuclear Engineering, Kansas State University, Manhattan, KS 66506, USA
[b] Radiation Detection Technologies, Inc., Manhattan, KS 66502, USA

ARTICLE INFO

Keywords:
^{3}He alternative
Neutron detection
Microstrip electrodes
Lithium foil
Radiation detector characterization

ABSTRACT

^{6}Li foils, each 75-μm thick, were positioned between a Schott Borofloat® 33 microstrip electrode and a planar drift electrode to construct suspended foil microstrip neutron detectors. MCNP6 simulations of two detector configurations, one containing a single ^{6}Li foil and the other containing five ^{6}Li foils, indicated expected maximum intrinsic thermal-neutron detection efficiencies of 18.36% and 54.08%, respectively. For comparison, the intrinsic thermal-neutron detection efficiency as a function of thermal-neutron beam position along the foil span was experimentally measured for both detector configurations. A non-uniform intrinsic thermal-neutron detection efficiency distribution was observed along the span of the ^{6}Li foil(s) between the microstrip and drift electrodes. Maximum intrinsic thermal-neutron detection efficiencies of 12.58 ± 0.15% and 29.75 ± 0.26% for the single and five ^{6}Li foils were measured, respectively. Gamma-ray rejection ratios of $6.46 \times 10^{-5} \pm 4.32 \times 10^{-7}$ and $7.96 \times 10^{-5} \pm 4.65 \times 10^{-7}$ were also measured, respectively, for a ^{137}Cs exposure rate of 50 mR h^{-1}. All measurements were conducted with the ^{6}Li foil(s) contained within a sealed aluminum enclosure pressurized with 10 psig of P-10 gas.

1. Introduction

The ^{3}He supply shortage (Kouzes, 2009; Shea and Morgan, 2010), resulting in an increase in the cost of ^{3}He, has motivated the development of several low-cost, high-efficiency, low-gamma-ray-sensitivity alternative technologies (Kouzes et al., 2010, 2015; Hurd and Kouzes, 2014). Multi-wire proportional counters (MWPC) with ^{6}Li-foils as neutron convertors were previously developed as a ^{3}He-alternative technology and these detectors had high intrinsic thermal-neutron detection efficiencies, ε_{th}, and low sensitivity to gamma rays (Nelson et al., 2011, 2012, 2014a, 2014b, 2015; Nelson, 2013). Reducing the size of ^{6}Li-foil MWPCs is limited due to a minimum space needed between neighboring ^{6}Li foils for anode wires. Likewise, the anode wires are susceptible to mechanical vibrations that induce microphonic noise. Suspended foil microstrip neutron detectors (SFMND) were developed (Edwards et al., 2016) by replacing the anode wires with a microstrip electrode (Oed, 1988). These detectors maintain the high ε_{th} of suspended ^{6}Li foils with the mechanical and electrical capabilities of microstrip electrodes (Fig. 1). SFMNDs are under development with the goal of producing a robust, low-cost, and compact ^{3}He-alternative technology capable of achieving high ε_{th} while maintaining low sensitivity to gamma rays.

Microstrip electrodes were previously utilized for a variety of neutron detection applications primarily relying on ^{3}He gas as the neutron conversion medium (Oed, 1988, 2004; Oed et al., 1989; Vellettaz et al., 1997; Clergeau et al., 2001; Takahashi et al., 2004; Fujita et al., 2007; Bateman et al., 2010, 2013). Studies were also performed using other neutron conversion media such as CsI-coated ^{6}Li and ^{157}Gd foils (Oed, 2004; Gebauer et al., 1998; Masaoka et al., 2003). However, bare ^{6}Li metals were not used because of the chemical reactivity of the material. ^{6}Li-based SFMNDs with one and five suspended 75-μm thick ^{6}Li foils using a silicon-based microstrip electrode were previously fabricated and tested (Edwards et al., 2016). Substantial differences between measured and simulated ε_{th} were observed, suspected to be due to microstrip electrode-based electrical phenomena (Edwards et al., 2016). Therefore, investigations into an electrically stable microstrip electrode substrate were conducted (Edwards et al., 2018). Schott Borofloat® 33 was identified as a low-cost, electrically stable microstrip electrode substrate that also reduced the capacitance from previously-used silicon-based microstrip electrodes (Edwards et al., 2018). The present work focuses on the optimization and refinement of ^{6}Li-based SFMNDs via the fabrication and neutron-sensitivity testing of ^{6}Li-based

* Corresponding author.
E-mail address: nedwards@ksu.edu (N.S. Edwards).

https://doi.org/10.1016/j.radphyschem.2018.02.013
Received 10 November 2017; Received in revised form 16 February 2018; Accepted 18 February 2018
Available online 19 February 2018
0969-806X/

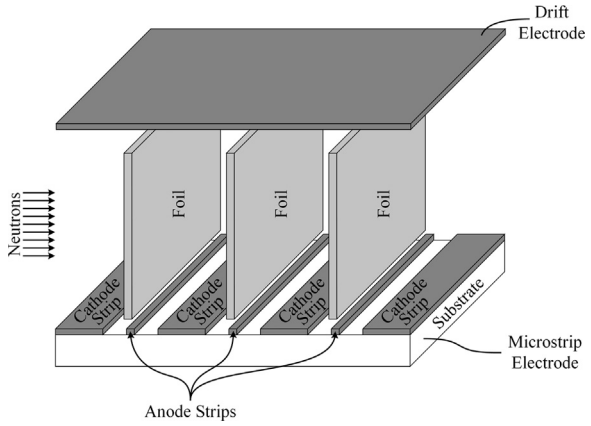

Fig. 1. Configuration of a SFMND depicting the orientation of suspended foils relative to microstrip and drift electrodes.

SFMNDs using a Schott Borofloat® 33 microstrip electrode.

2. Theoretical considerations

Neutron detection using the ^{6}Li-based SFMND occurs in three main steps, as depicted in Fig. 2: 1.) neutron conversion, 2.) drift of charge carriers, and 3.) charge multiplication. The first step occurs when an incident slow neutron is absorbed by a ^{6}Li atom with a microscopic thermal-neutron absorption cross-section of 940 b (Knoll, 2010; Tsoulfanidis, 1995; McGregor et al., 2003). The ensuing ^{6}Li(n,α)^{3}He reaction, with a total reaction *Q*-value of 4.78 MeV, yields reaction products that are emitted in opposite directions with energies described by,

$$ {}_{0}^{1}n + {}_{3}^{6}Li \rightarrow {}_{2}^{4}He(2.05\ MeV) + {}_{1}^{3}H(2.73\ MeV). \quad (1) $$

Although the thermal-neutron absorption cross-section of ^{6}Li is lower than ^{10}B (3840 b) (Knoll, 2010; Tsoulfanidis, 1995; McGregor et al., 2003), the reaction *Q*-value is significantly higher than that of ^{10}B (2.31 MeV). This increase in reaction *Q*-value allows for sufficient discrimination of background radiation and gamma rays without significantly sacrificing neutron-detection performance.

Upon exiting the ^{6}Li foil and entering the backfill gas, the reaction products ionize the backfill gas resulting in the liberation of charge carriers. The second step in the detection process occurs when the potential difference between the drift electrode voltage, V_d, and the microstrip anode and cathode strip voltages, V_a and V_c, respectively, cause charge carriers to drift through the gas within the drift electric field. The operating voltage condition of $V_d < V_c < V_a$ is required to drift electrons towards the microstrip electrode surface and positively-charged ions towards the drift electrode. Therefore, the second step of the detection process is equivalent to the signal formation process that occurs in a parallel-plate ionization chamber. When electrons approach the microstrip electrode surface, the electric field strength increases by

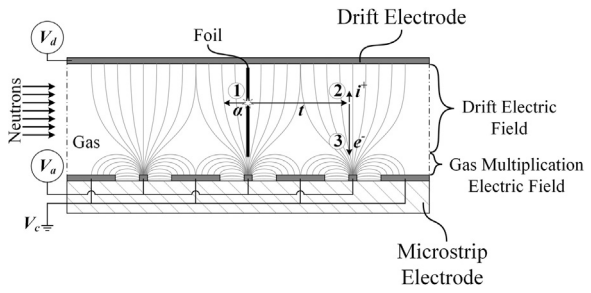

Fig. 2. Three-step neutron detection process for suspended ^{6}Li foil(s) positioned between a drift electrode and a microstrip electrode.

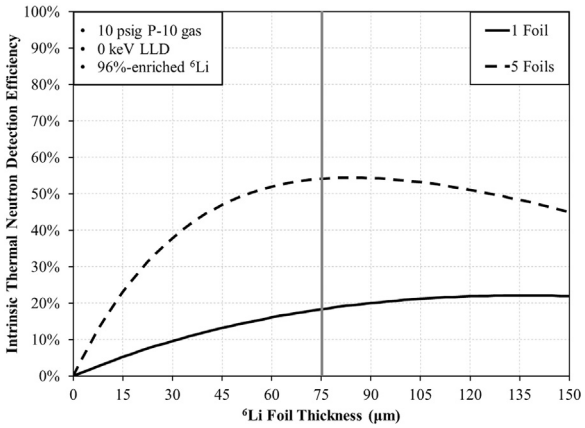

Fig. 3. MCNP6-simulated ε_{th} curves as a function of ^{6}Li foil thickness for one and five foils in 10 psig (1.68 atm) of P-10 proportional gas. The foils were assumed to be 96%-enriched ^{6}Li and the ε_{th} curves are plotted for a LLD setting of 0 keV.

several orders of magnitude and surpasses the critical electric field strength necessary to cause Townsend avalanching, denoted in Fig. 2 as the gas multiplication electric field region. This increase in electric-field strength occurs as a result of the potential difference between neighboring anode and cathode strips positioned less than 1.0 mm apart, where $V_a > V_c$. Furthermore, the difference in anode and cathode strip width provides a geometric weighting condition that further enhances the electric field strength beyond the potential difference between neighboring anode and cathode strips. Thus, the third step in the neutron detection process occurs at this electric-field boundary where gas multiplication can occur.

The ε_{th} as a function of ^{6}Li foil thickness for SFMNDs containing one and five foils was simulated using MCNP6 as shown in Fig. 3. A lower level discriminator (LLD) setting of 0 keV was used when generating the ε_{th} curves to determine the maximum ε_{th} as a function of foil number and thickness. P-10 proportional gas (90% argon, 10% methane) pressurized to 10 psig (1.68 atm) was backfilled into a chamber with 96%-enriched ^{6}Li foils. For 75-μm thick ^{6}Li foils, theoretical ε_{th} of 18.36% and 54.08% are predicted for a chamber with one and five foils, respectively. Simulated reaction-product pulse-height spectra, corresponding to the left *y*-axis with units of "counts/source neutron", for one and five ^{6}Li foils are shown in Fig. 4. The simulated ε_{th} shown in Fig. 4, corresponding to the right ordinate, indicates the change in neutron-detection performance as a function of LLD setting. Thus, as the prominence of the simulated reaction-product spectral features increases, the simulated ε_{th} decreases.

The difference in pulse-height spectra features shown in Fig. 4 is a consequence of differences in foil positions coupled with differences in interaction location, reaction-product particle ranges, and their corresponding particle trajectories (Nelson, 2013; Nelson et al., 2014a). Four reaction-product emission scenarios exist, as previously reported in literature (Nelson, 2013; Nelson et al., 2014a), based on the range in pure ^{6}Li foil of the 2.05 MeV alpha particles and 2.73 MeV tritons of 23.2 μm and 133 μm, respectively (Nelson, 2013; Nelson et al., 2014a; Ziegler and Biersack, 2013). The ranges of the 2.05 MeV alpha particle and 2.73 MeV triton are 7.50 mm and 43.2 mm, respectively, in 10 psig of P-10 proportional gas (Ziegler and Biersack, 2013). The single-foil scenario was simulated with the foil positioned 1-mm laterally off-center within the drift electric field region, as shown in Fig. 5. As a result, a minimum distance of approximately 20–21 mm, perpendicular to the foil surface, exists between the foil surface and the perimeter of the drift electric field region. The perimeter of the drift electric field region is defined by the perimeter of the microstrip electrode.

As illustrated in Fig. 5, assuming reaction products with full energy are emitted into the backfill gas perpendicular to the foil surface, the alpha-particle energy will be fully absorbed within the drift electric